

Preparation and Characterization of PVA Films with Magnetic Nanoparticles: The Effect of Particle Loading on Drug Release Behavior

Paula Bertoglio,¹ Silvia E. Jacobo,¹ Marta E. Daraio²

¹Laboratorio de Físicoquímica de Materiales Cerámicos Electrónicos, Departamento de Química, Universidad de Buenos Aires, Av. Paseo Colón 850, C1063ACV, Buenos Aires, Argentina

²Grupo de Aplicaciones de Materiales Biocompatibles, Departamento de Química, Facultad de Ingeniería, Universidad de Buenos Aires, Av. Paseo Colón 850, C1063ACV, Buenos Aires, Argentina

Received 1 March 2009; accepted 21 August 2009

DOI 10.1002/app.31315

Published online 7 October 2009 in Wiley InterScience (www.interscience.wiley.com).

ABSTRACT: This article deals with the drug release behavior of theophylline (Th) from poly(vinyl alcohol) (PVA) hydrogels, prepared with magnetic nanoparticles at different particle loadings. These biocompatible matrices were obtained by incorporating different amounts of an aqueous ferrofluid into PVA hydrogels, loaded with Th as a marker for drug-delivery studies. PVA films with magnetic particles proved to be magnetic field-responsive materials as the drug release decreased through the application of a relative low and uniform magnetic field for particle concentrations of 0.9% w/w or higher. Moreover, the percentage of restriction of drug release is found to be correlated with particle load-

ing. The *in vitro* release profiles were analyzed by applying a semiempirical power law to obtain the kinetic parameters. The value of the release exponent was found to be in the range 0.54–0.56 in all experiments, which thus indicates a predominant diffusional mechanism for drug release from these smart magnetic hydrogels. This effect suggests the possibility of modulating the release behavior by controlling the particle content in the preparation of the composites. © 2009 Wiley Periodicals, Inc. *J Appl Polym Sci* 115: 1859–1865, 2010

Key words: polyvinyl alcohol; stimuli-sensitive polymers; drug-delivery systems; nanoparticles; ferrofluids

INTRODUCTION

Environmentally sensitive hydrogels for controlled release of drugs have received great consideration in recent years. Many previous studies have been reported about response to specific stimuli, such as temperature,^{1,2} pH,^{3,4} and electric field.⁵ Zrínyi et al.^{6,7} reported a magnetic-field-sensitive gel named ferrogel that combines the magnetic properties of magnetic fillers and the elastic properties of hydrogels. This material is a chemically crosslinked polymer network swollen by a colloidal dispersion of monodomain magnetic particles of about 10 nm with superparamagnetic behavior (ferrofluid). Biodegradable gels that change in shape under the influence of an external magnetic field have also been synthesized using hydroxypropylcellulose and maghemite.⁸

Magnetic hydrogels suitable for drug release applications were prepared by chemically crosslinking of gelatin hydrogels and magnetite nanoparticles

using genipin as a crosslinking agent.^{9,10} *In vitro* release data showed that through the application of magnetic fields to the magnetic hydrogels, the release rate of the drug included in the hydrogels was significantly restricted when compared with those when the field was turned off.⁹

Polyvinylalcohol (PVA) is a well-known biocompatible polymer that has received great attention because of its good gel and film forming properties. These characteristics explain its broad use for biomedical purposes.¹¹ The preparation of PVA magnetic films from an aqueous ferrofluid has been reported.¹² In a recent paper, we presented results on biocompatible composites that were prepared by incorporating a ferrofluid into PVA and scleroglucan hydrogels loaded with Theophylline (Th) as a model drug, where the amount of drug released from the polymeric composite was efficiently decreased under the influence of an external magnetic field.¹³

In this work, we studied films of PVA chemically crosslinked with glutaraldehyde, added with a stabilized magnetite sol at different particle loadings, to evaluate the influence on *in vitro* drug release behavior of a preparation condition such as particle content. These matrices are studied with the purpose of evaluating them as possible magnetic responsive delivery materials suitable for controlled release devices.

Correspondence to: M. E. Daraio (medit@fi.uba.ar).

Contract grant sponsor: Universidad de Buenos Aires; contract grant numbers: Projects UBACyT I011, I013.

EXPERIMENTAL

Materials

The PVA used (Riedel-de Haën, Hanover, Germany) had an average molecular weight (M_w) of 22,000 and a saponification value of 87%. Glutaraldehyde (GTA) solution (25% w/w) was purchased from J.Baker (Phillipsburg, NJ). Th (Theophylline, $C_7H_8N_4O_2$, $M_w = 180.17$), in conformity with British Pharmacopeia standards, was provided by Saporiti Laboratories (Buenos Aires, Argentina). Th was chosen as the model drug for release studies due to its sensitive detection by UV absorption (271 nm) and its stability in aqueous solution, and it was present in all preparations at 0.2% w/w. The surfactant cetyltrimethylammonium bromide (CTAB) was purchased from Sigma (St. Louis, MO). All other chemicals were reagent grade and used without further purification.

Methods

Preparation of ferrofluid

The magnetic ferrofluid was prepared in water from magnetic nanoparticles and the cationic surfactant CTAB. The detailed synthesis of magnetite (Fe_3O_4) from iron chloride ($FeCl_2$ and $FeCl_3$) in aqueous solution was described earlier.¹² An aqueous dispersion of magnetic nanoparticles was prepared by alkalizing with diluted ammonia to maintain an anionic charge on the particle surface. Then, an aqueous solution of CTAB was added and the samples were sonicated for 3 h. The optimum surfactant concentration to prepare a stable ferrofluid was selected taking into account the maximum % w/v of Fe_3O_4 obtainable in the ferrofluid.¹⁴

Preparation of PVA magnetic films containing Th

PVA composites were prepared at $(25 \pm 2)^\circ C$ by using the aqueous ferrofluid previously sonicated for 15 min and adding it to PVA and Th solutions. Magnetic particles loadings were 0, 0.3, 0.9, and 1.5% w/w in the different samples. Final PVA and Th concentrations were kept constant in the hydrogels at 4.0% and 0.2% w/w, respectively. A GTA solution was used as the crosslinking agent to form the gel. The degree of crosslinking (moles of monomer units per mol of crosslinking agent) was 500 in all preparations. PVA films were obtained by maintaining the ferrogels in Petri dishes at low humidity in a sealed container with silica gel for 1 week.

A low GTA concentration was used to protect the biocompatibility of the PVA gel, minimizing the residual aldehyde.¹³

Characterization of nanoparticles and ferrofluid

The structural properties of the nanoparticle powders were analyzed by X-ray powder diffraction (XRD)

with a Rigaku (Tokyo, Japan) diffractometer using a $Cu K_\alpha$ radiation. The average size of the crystals was estimated using Scherrer's equation.¹⁵ The magnetic properties were carried out using a Quantum Design (San Diego, CA) MPMS Squid magnetometer. The zero-field-cooled (ZFC) and field-cooled (FC) measurements were performed by cooling the nanoparticles to 10 K at zero field or in the presence of an external field of 50 Oe. The hysteretic loops for a stable ferrofluid were measured at room temperature.

Mössbauer effect (ME) spectroscopy was performed under transmission geometry at constant acceleration mode with a $^{57}CoRh$ radioactive source. Isomer shifts (δ) are referred to room temperature α -Fe. The spectra were fitted with Lorentzian curves or with histograms of Lorentzian curves.

Environmental scanning electron microscopy (ESEM)

The surface morphology of the PVA hydrogels was observed by ESEM. Micrographs of PVA matrices were obtained using an ESEM 2010 (FEI Company, Hillsboro, OR) microscope. The electron beam had a voltage of 20 kV.

Drug release measurements

Th-release assessments of composites were performed in a Flat Ground Joint type Franz Cell (PermeGear, Hellertown, PA). A Franz cell has two vertical compartments. The PVA composite is placed in the upper donor chamber, and the lower receptor compartment is initially filled with distilled water. In the lower compartment, the Th concentration increases as drug release occurs and samples are taken at different times. A membrane of cellulose was placed between the upper section of the Franz cell and the lower receptor compartment sustaining the material being tested.

To test the magnetic effect on drug-delivery pattern, a magnetic field of 600 G was applied on the donor compartment of the Franz cell, with magnetic field lines parallel to the release surface of the sample. The PVA film sample was placed between the magnetic poles in a region with homogeneous field.

The kinetic experiments were performed under thermostatic control ($25^\circ C$). Because of the magnetic nature of the samples, the constant stirring of the receptor chamber was achieved using a mechanical stirrer. Measurements of drug concentration were performed by taking samples (200 μL) with a syringe at fixed times from the sampling port of the receptor compartment. The Th absorbance was measured at 271 nm in a Shimadzu UV-2401 spectrophotometer (Shimadzu, Kyoto, Japan). After each aliquot was taken, the volume (20 mL) in the receptor compartment was filled with distilled water, assuring a

constant volume and a full contact between the polymeric matrix supported by the membrane and the receptor liquid.

Drug release data handling

Taking into consideration that the surface of the sample in contact with the liquid of the receptor compartment of the Franz diffusion cell is the only available area for drug release, a one-dimensional release process was assumed. The cumulative concentration of Th released was calculated from a calibration plot (molar absorption coefficient of Th at 271 nm in water = $1.0 \times 10^4/M$ cm). For each set of experimental conditions, data from replicated experiments were plotted as a group. The data were fitted only at short times (upto 8000 s) to preserve an almost ideal sink condition, which is low-drug concentration in the release medium. Curves of Th concentration (C_t) as a function of time (t) were plotted and the cumulative concentration of Th was adjusted to a power-law type relationship^{16,17}:

$$m_t/m_\infty = k t^n \quad (1)$$

Here, m_t and m_∞ are the cumulative amount of drug released after a time t and an infinite time, respectively, k is a constant related to kinetic behavior and experimental conditions, and n is the exponent depending on the release process. Both m_∞ and k were incorporated in a constant K , and eq. (2) was used to fit the data:

$$C_t = K t^n \quad (2)$$

where C_t is the molar concentration of Th in the receptor compartment at time t . A global analysis of different replicate experiments by nonlinear least-squares procedure using Matlab was applied.¹⁸

RESULTS AND DISCUSSION

Nanoparticles and ferrofluid characterizations

XRD patterns (not shown¹⁴) for the magnetic nanoparticles dried from a stable ferrofluid indicate that Fe_3O_4 is the main phase, although $\gamma\text{-Fe}_2\text{O}_3$ (maghemite) cannot be disregarded. The average crystal sizes determined by Scherrer's equation¹⁵ with XRD data have been found in a range of (4.0 ± 0.2) nm. This low-crystalline size indicates a superparamagnetic system. This behavior is observed in ZFC-FC loops (Fig. 1) where the magnetization (M) dependence on the temperature (T) of nanoparticles dried from a stable ferrofluid exhibits a cusp around 120 K in the ZFC branch and a blocking temperature T_B determined from the branching of the ZFC and FC

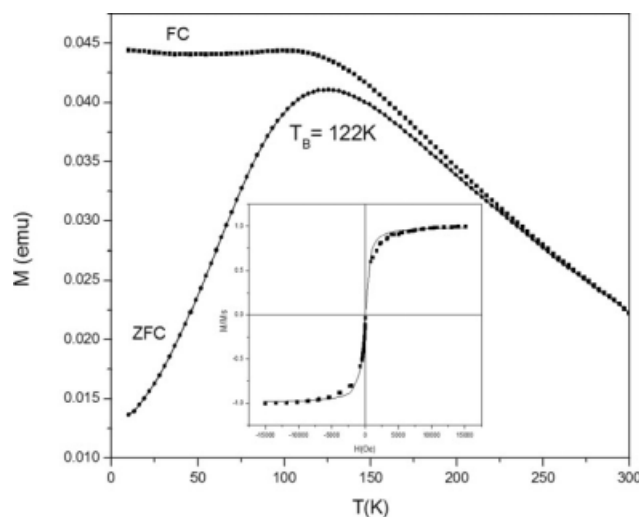


Figure 1 Magnetization vs. temperature measured at 50 Oe in the zero-field-cooled and field-cooled states (ZFC-FC) for nanoparticles dried from a stable ferrofluid. Inset: reduced magnetization as a function of applied magnetic field for a stable ferrofluid at room temperature.

data. The ZFC curve splits from the FC curve at around 175 K. Above T_B , superparamagnetic particles become thermally unstable and the magnetization decreases as MV_i/kT (V_i : particle volume; k : Boltzmann constant) becomes larger than 1. When the particles are physically coated by the surfactant (CTAB), agglomeration is avoided as the surfactant-coated nanoparticles are freely aligned with the external field and the repulsive force between cationic surfactant molecules coated on single particles can prevent agglomeration.¹⁹

The inset of Figure 1 shows the reduced magnetization (M/M_s) loop of the ferrofluid as a function of the applied magnetic field (H) at room temperature. This profile indicates superparamagnetic behavior, as evidenced by zero coercivity and remanance on the magnetization loop. To describe the magnetization of the magnetic fluid, several theoretical models are used, but the simplest one is Langevin's model.¹⁵

Assuming that the iron oxide particles exhibit superparamagnetic behavior and that the volume fraction is below 1%, the magnetization variation as a function of magnetic field can be described by the Langevin equation:

$$M = M_s [\coth(\mu H/kT) - kT/\mu H] \quad (3)$$

where M and M_s are the magnetization and the saturation magnetization (emu cgs), respectively, μ is the magnetic moment of each particle (emu cgs), H is the magnetic field (Oe), T is the absolute temperature, and k is the Boltzmann constant. The Langevin relation considers each particle as a magnetic monodomain. The inset of Figure 1 shows the best fit to

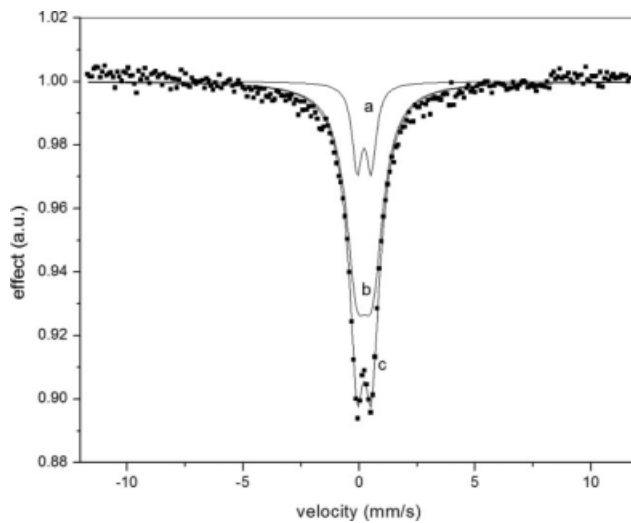


Figure 2 Mössbauer spectra at room temperature of magnetic nanoparticles dried from a stable ferrofluid fitted with two quadrupole doublets (a, b). Experimental values are shown (c).

eq. (3). From this data fitting, the mean-magnetic moment per particle of sample is found to be $1672 \mu_B$.

It is also possible to determine the standard deviation and median particle diameter from the room temperature magnetization measurements using a method proposed by Chantrell et al.,²⁰ using the following:

$$D_m = \left[(18kT/\pi M_b) (\overline{\chi}_i/3H_0)^{1/2} \right]^{1/3} \quad (4)$$

and

$$\sigma_m = \frac{1}{3} [\ln(3\overline{\chi}_i H_0)]^{1/2} \quad (5)$$

where D_m : median magnetic diameter of the log normal volume distribution,

σ_m : standard deviation of the log D_m ,

M_b : bulk saturation magnetization of the particles/unit volume (=Ms. ρ),

$\overline{\chi}_i$: reduced initial susceptibility ($\overline{\chi}_i = \chi_i/M_s$),

$1/H_0$: point where the extrapolation of M versus $1/H$ curve crosses the $M = 0$ axis.

For our system, $M_s = 18.5 \text{ emu/g}$ and ρ is the theoretical density of the iron oxide ($\approx 5.1 \text{ g/cm}^3$). In eq. (4) the value D_m depends on the value of M_b . In eqs. (4) and (5), one uses magnetic measurements in low and high fields to obtain a fit to a sum of Langevin functions. In these fluids, particle interactions, especially for larger particles, can greatly influence the values of D_m and σ_m using this method. The magnetic particle size calculated by eq. (4) was $D_m = 6.0 \text{ nm}$ and the standard deviation of the diameter from eq. (5) was $\sigma_m = 0.42$.

Mössbauer spectra of the nanoparticles dried from a stable ferrofluid are shown in Figure 2. The spectra were fitted with two quadrupole doublets with isomer shifts (δ) of 0.31 and 0.33 mm/s and with relatively high quadrupole splittings (ΔE_Q) of 0.69 and 0.69 mm/s, respectively. Distorted coordination symmetry at the surface of small particles can produce high quadrupole shift in the spectra. These values are characteristic of nanometer-size superparamagnetic iron oxide particles above their blocking temperature (Fig. 1).²¹

Surface morphology of films

In an attempt to explore the sample morphology, ESEM micrographs were obtained. Figures 3 and 4 correspond to PVA matrix without or with 0.3% w/w of magnetite particles, respectively. Figure 3 shows a micrograph of a PVA film with pores of about $5.6 \mu\text{m}$. From Figure 4, it can be seen that the magnetic particles agglomerate forming structures of about $2\text{--}3 \mu\text{m}$ and are distributed in a compact PVA matrix. The identical magnification (scale bar: $50 \mu\text{m}$) selected for both micrographs allows the denser structure of the composite film to be observed. Similar morphologies were observed for other particle loadings (ESEM not shown).

Drug delivery

The drug release behavior of PVA magnetic gels, with and without the application of an external magnetic field, is shown in Figures 5–7.

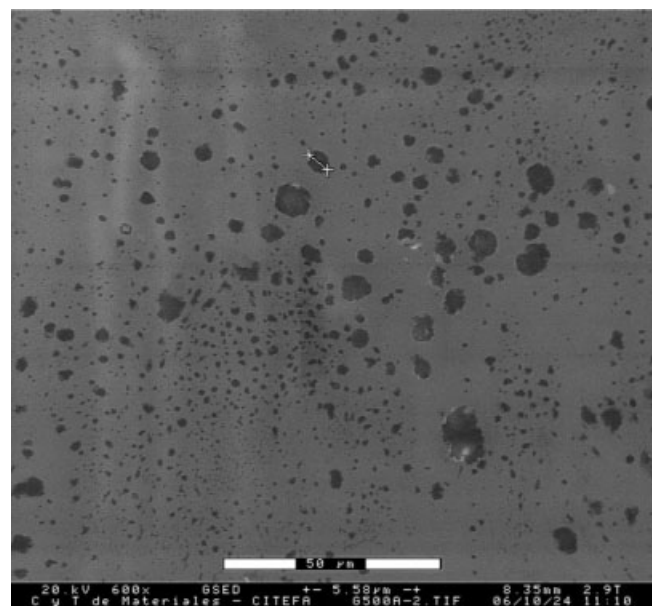


Figure 3 ESEM micrograph of a 4% w/w PVA film without magnetic particles. Conditions: electron beam voltage 20 kV, amplification $\times 600$, 8.35 mm working distance, 2.9 Torr water vapor pressure.

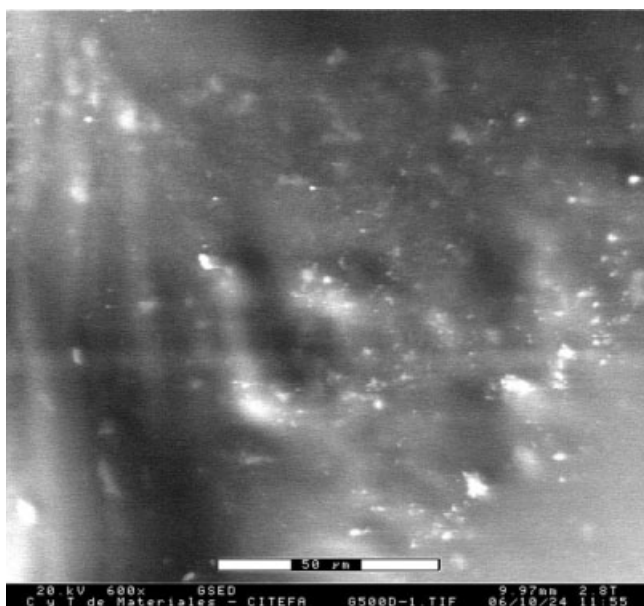


Figure 4 ESEM micrograph of a 4% w/w PVA film with 0.3% w/w of magnetite particles. Conditions: electron beam voltage 20 kV, amplification $\times 600$, 9.97 mm working distance, 2.8 Torr water vapor pressure.

The curve included in Figure 5 was obtained for PVA samples containing 0, 0.3, 0.9, and 1.5% w/w of magnetic particles, in the absence of external magnetic field. These results indicate that the presence of magnetic particles does not modify the release pattern of PVA gel, when a magnetic field is not applied. Thus, it can be considered that, at least for drug release applications, the structure of the gel is not greatly disturbed by nonoriented particles, in the range of the used concentrations.

Figure 6 compares the response of PVA gels containing 0.9% and 1.5% w/w of magnetic particles when an external magnetic field of 600 G is applied from the beginning of the experiment and the behavior with no magnetic field (upper curve). The material with 1.5% of particles shows a 36% reduction in the concentration of drug released at 7000 s compared with the release pattern in the absence of applied field. When 0.9% w/w of magnetic particles is included in the gel it can be appreciated that the application of the magnetic field produces a 23% decrease in the concentration of Th delivered at 7000 s compared with the upper curve obtained for the same material without an applied magnetic field. Figure 7 illustrates the release pattern for a particle loading of 0.3% w/w. A different behavior can be observed as the application of an external magnetic field does not produce any measurable effect on the release curve. These results point toward the possibility of modulating the effect of the applied magnetic field by controlling the amount of ferrofluid loaded in the gel.

It is interesting to compare these observations with those recently obtained in our laboratory for a related PVA composite using a PVA gel with a crosslinking degree (moles of monomer units per mol of crosslinking agent) of 200.¹³ In that work, up to 2100 s from the beginning of the experiment, the sample showed the same drug release profile with or without a magnetic field of 600 G. At 2100 s, both curves started to come apart due to the magnetic effect on drug delivery, showing an appreciable orientation time for the magnetic particles. In this work, the crosslinking degree of PVA is 500, leading to a lower firmness of the hydrogel. This condition allows the magnetic effect to be observed from the beginning of the release.

To understand the effect of applied field on composite polymeric matrices, we relate the observed results to previous work where we reported rheological experiments measuring the elastic modulus G' for a scleroglucan composite.¹³ It has to be mentioned that the G' value can be used as an indicator of hardness.²² To test the influence of the magnetic field on G' , we placed the scleroglucan-magnetite material under an external uniform field of 600 Gauss during 20 or 69 h before the rheological test. A 20-h treated material (exposed to magnetic field) showed a 30% increase in the G' modulus when compared with the value obtained for the untreated one. An increase of 95% was observed in G' when comparing a 20-h treated system with a 69-h treated one, indicative of a bigger rigidity of the matrix resulting from the magnetic field exposure.¹³

In addition, a higher rigidity-lower drug release correlation can be proposed from previous results where an increased elastic modulus G' with growing

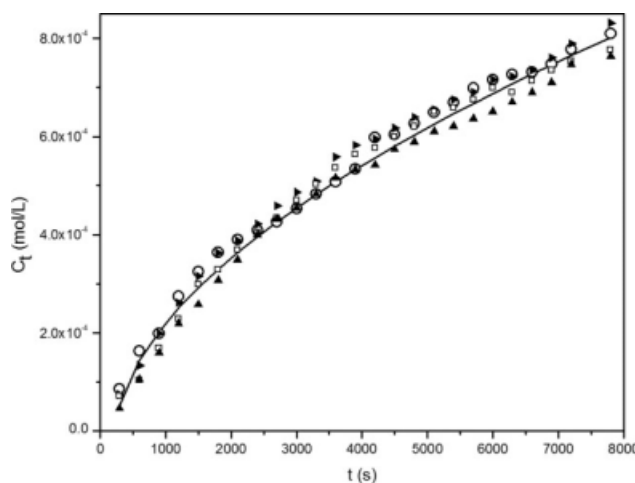


Figure 5 Cumulative concentration of Th as a function of release time without applied magnetic field, for PVA composites with: (○) 0% w/w Fe₃O₄; (▴) 0.3% w/w Fe₃O₄; (▲) 0.9% w/w Fe₃O₄; (□) 1.5% w/w Fe₃O₄. Line represents calculated values according to eq. (2). Best fit parameters were taken from Table I.

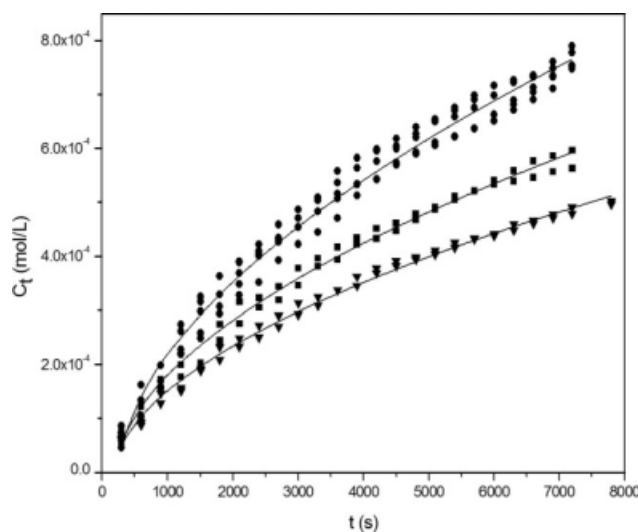


Figure 6 Cumulative concentration of Th as a function of release time, for PVA gels: (●) with 0.9 or 1.5% w/w Fe₃O₄ without applied magnetic field; (■) with 0.9% w/w Fe₃O₄ and an applied magnetic field of 600 G; (▼) with 1.5% w/w Fe₃O₄ and an applied magnetic field of 600 G. Lines represent calculated values according to eq. (2). Best fit parameters were taken from Table I.

polymer concentration (more solid matrix) was observed concomitantly with a significantly lower drug release.²³

For release data treatment, it was determined that our data were best fitted by the power-law model taking into account the existence of an initial lag-time of about 200 s for all experiments. This preliminary time could be interpreted as an initial delay in attaining a definite release behavior and was subtracted from the experimental time data before the fitting to eq. (2). This equation can be considered as an expression that takes into account two independent mechanisms of drug transport, a Fickian diffusional release due to a chemical potential gradient and a relaxational release due to water penetration into the system (the rate-determining step being the relaxation process of the macromolecules). Accordingly, for slab geometry, the n parameter in eq. (2) has two characteristic values with physical significances: $n = 0.5$ (diffusion-controlled drug release) and $n = 1.0$ (relaxation-controlled drug release).¹⁷ Values of n between 0.5 and 1.0 can be considered as a combination of the two mechanisms mentioned earlier. Table I presents the results of kinetic parameters from eq. (2) fitting, for samples containing 0, 0.3, 0.9, and 1.5% w/w of magnetic particles, in the absence or in the presence of external magnetic field. Data are properly described by this equation, as can be appreciated in the curves of Figures 5–7 and as is revealed by the square correlation coefficients (R^2) ranging from 0.9847 to 0.9942 in Table I. The values of n , the release exponent, are in the range 0.54–0.56

in all experiments and indicate a predominant diffusional control for drug release.

The drug-delivery behavior can be affected by two different morphological characteristics of the PVA films: the pore size and the tortuosity of the inner pore channels. ESEM micrographies show a denser gel structure when nanoparticles are included, even for 0.3% w/w of particles (Figures 3 and 4), suggesting a pore size decrease. Considering the drug size (Th radius 3.8 Å)²⁴ and the huge difference with pores in the order of micrometers, it is expectable that a moderate decrease in pore size in the denser structure shown in Figure 4 does not modify the release of the drug. Another topic to be considered is the particle volume fraction employed in these experiments, which is in the order of 0.004 for the higher particle concentration (1.5% w/w). We propose that this low-volume fraction of randomly distributed particles (without applied magnetic field) may not be acting as a physical barrier to perturb the diffusion of the drug. Figure 5 is in agreement with the previous analysis.

In the presence of magnetic field, an increased tortuosity of the inner channels resulting from the formation of particle chains could be proposed, in agreement with the results reported by Liu et al.²⁵ Tortuosity is used to account for the increase in distance a diffusing molecule travels due to twisting or distortion of pores and can be defined as the ratio of the actual path length through the pores to the shortest linear distance.²⁶ For hydrogels, when pore sizes are much larger than the molecular dimensions of the drug, the diffusion coefficients are inversely related to the tortuosity of the gel.²⁷ Therefore, an increased tortuosity of the matrix points to a slower

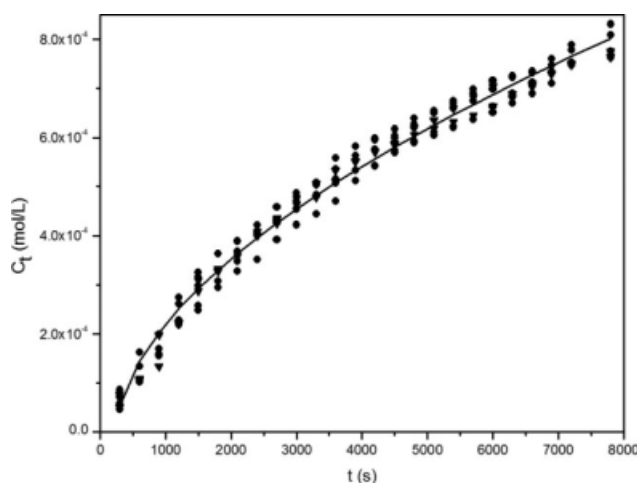


Figure 7 Cumulative concentration of Th as a function of release time, for PVA composites with 0.3% w/w Fe₃O₄: (●) without or (▼) with applied magnetic field of 600 G. Line represents calculated values according to eq. (2). Best fit parameters were taken from Table I.

TABLE I
Drug Release Kinetic Parameters^a Obtained for PVA-Magnetite Films at 25°C

% w/w Fe ₃ O ₄	Magnetic field	<i>n</i> ^b	<i>K</i> ^b (mol L ⁻¹ s ⁻ⁿ)	<i>R</i> ²
0; 0.3; 0.9; 1.5	Not applied	0.56 ± 0.02	(5.2 ± 1.0) × 10 ⁻⁶	0.9847
0.3	Applied	0.54 ± 0.02	(6.2 ± 1.3) × 10 ⁻⁶	0.9901
0.9	Applied	0.55 ± 0.03	(4.7 ± 1.2) × 10 ⁻⁶	0.9914
1.5	Applied	0.55 ± 0.02	(3.9 ± 0.8) × 10 ⁻⁶	0.9942

^a Mean and confidence intervals are informed. All parameters are within the 95% confidence interval of the nonlinear least square estimate.

^b Kinetic parameters were obtained by fitting the data through eq. (2).

drug release. The effect of magnetic particles becomes perceptible in drug delivery only for magnetite concentrations of 0.9% w/w or higher and through the application of an external magnetic field. We propose that the magnetic field leads to the formation of particle chain arrangements, oriented structures that give additional rigidity and increased tortuosity to the matrix giving a decreased drug release.

CONCLUSIONS

Biocompatible PVA composite magnetic gels containing different amounts of magnetic particles and loaded with theophylline were successfully prepared and tested as drug-delivery matrices. The structural and magnetic properties of the ferrofluid were analyzed by X-ray powder diffraction and a Quantum Design MPMS Squid magnetometer.

PVA films with magnetic particles (0.9 % w/w or higher) proved to be magnetic field-responsive materials as the drug release kinetics can be decreased by the application of a relative low and uniform magnetic field. This effect could be related to an increased tortuosity of the inner channels resulting from the formation of particle chains under the influence of the magnetic field.

The important point is that the percentage of restriction of drug release is found to be correlated with particle loading. This effect suggests the possibility of modulating the release behavior by controlling the particle content in the preparation of the composites. It has to be mentioned that depending on the desired drug effect, a reduced-drug delivery could be a benefit. For example, a decreased release rate would allow a larger time window for drug liberation.

The reported results suggest that these PVA-Fe₃O₄ composites are smart magnetic materials showing potential for their application in novel drug-delivery systems responsive to environmental stimuli, like external magnetic field.

References

- Eeckman, F.; Möes, A. J.; Amighi, K. *Int J Pharm* 2004, 273, 109.
- Zhang, X. Z.; Wu, D. Q.; Chu, C. C. *Biomaterials* 2004, 25, 3793.
- Chen, S. C.; Wu, Y. C.; Mi, F. L.; Lin, Y. H.; Yu, L. C.; Sung, H. W. *J Controlled Release* 2004, 96, 285.
- Pardini, O.; Amalvy, J.; François, N. J.; Daraio, M. E. *J Appl Polym Sci* 2007, 104, 4035.
- Shang, J.; Shao, Z.; Chen, X. *Biomacromolecules* 2008, 9, 1208.
- Zrínyi, M.; Barsi, L.; Büki, A. *J Chem Phys* 1996, 104, 8750.
- Zrínyi, M.; Barsi, L.; Büki, A. *Polym Gels Networks* 1997, 5, 415.
- Chatterjee, J.; Haik, Y.; Chen, C. J. *Colloid Polym Sci* 2003, 281, 892.
- Liu, T. Y.; Hu, S. H.; Liu, K. H.; Liu, D. M.; Chen, S. Y. *J Magn Magn Mater* 2006, 304, e397.
- Hu, S. H.; Liu, T. Y.; Liu, D. M.; Chen, S. Y. *Macromolecules* 2007, 40, 6786.
- Scotchford, C. A.; Cascone, M. G.; Downes, S.; Giusti, P. *Biomaterials* 1998, 19, 1.
- Albornoz, C.; Jacobo, S. E. *J Magn Magn Mater* 2006, 305, 12.
- François, N. J.; Allo, S.; Jacobo, S. E.; Daraio, M. E. *J Appl Polym Sci* 2007, 105, 647.
- Bertoglio, P.; Daraio, M. E.; Jacobo, S. E. In *Actas del XXII Congreso Interamericano de Ingeniería Química—V Congreso Argentino de Ingeniería Química*; Buenos Aires, 2006; ISSN: 1850 3519 (CAIQ) y 1850 3535 (CIQ).
- Cullity, B. D. *Elements of X-ray Diffraction*; Addison-Wesley: Reading MA, 1987.
- Ritger, P. L.; Peppas, N. A. *J Controlled Release* 1987, 5, 23.
- Ritger, P. L.; Peppas, N. A. *J Controlled Release* 1987, 5, 37.
- Matlab version 7.5; The MathWorks, Inc.: Natick, Massachusetts 2007.
- Lin, X. M.; Sorensen, C. M.; Klabunde, K. J.; Hadjipanayis, G. C. *Langmuir* 1998, 14, 7140.
- Chantrell, R. W.; Poplewell, J.; Charles, S. W. *IEEE Trans Magn* 1978, MAG-14, 975.
- Kundig, W.; Bommel, H.; Konstabaris, G.; Lundquist, R. *Phys Rev* 1966, 142, 327.
- Narine, S.; Marangoni, A. *Lebensmittel Wiss Technol* 2001, 34, 33.
- François, N. J.; Rojas, A. M.; Daraio, M. E.; Bernik, D. L. *J Controlled Release* 2003, 90, 355.
- Amsden, B. *Macromolecules* 1998, 31, 8382.
- Liu, T. Y.; Hu, S. H.; Liu, T. Y.; Liu, D. M.; Chen, S. Y. *Langmuir* 2006, 22, 5974.
- Wu, Y. S.; Van Vliet, L. J.; Frijlink, H. W.; Van Der Voort Maarschalk, K. *Eur J Pharm Sci* 2006, 28, 433.
- Peppas, N. A. *Hydrogels in Medicine and Pharmacy*; CRC Press: Boca Raton, FL, 1986; Vol. 1–3, p 180.